Received: 15 May 2023 | Revised: 7 November 2023 | Accepted: 4 December 2023

DOI: 10.1002/joc.8339

International Journal of Climatology RMetS

RESEARCH ARTICLE

Evaluation of ERA5 precipitation and 10-m wind speed associated with extratropical cyclones using station data over North America

Ting-Chen Chen[1,2] | **François Collet**[1,3] | **Alejandro Di Luca**[1]

[1]Département des Sciences de la Terre et de l'atmosphère, Centre Étude et simulation du climat à l'échelle régionale (ESCER), Université du Québec à Montréal, Montréal, Quebec, Canada

[2]Institute for Meteorology and Climate Research—Department Troposphere (IMK-TRO), Karlsruhe Institute of Technology, Karlsruhe, Germany

[3]CECI Université de Toulouse, CERFACS/CNRS, Toulouse, France

Correspondence
François Collet, CECI Université de Toulouse, CERFACS/CNRS, Toulouse, France.
Email: collet@cerfacs.fr

Funding information
Natural Sciences and Engineering Research Council of Canada (NSERC), Grant/Award Number: RGPIN-2020-05631; Government of Québec

Abstract

While the ERA5 reanalysis is commonly utilized in climate studies on extratropical cyclones (ETCs), only a few studies have quantified its ability in the representation of ETCs over land. To address this gap, this study evaluates ERA5's skill in representing the ETC-associated 10-m wind speed and the precipitation in central and eastern North America during 2005–2019. Hourly data collected from ∼3000 stations, amounting to around 420 million reports stored in the Integrated Surface Database, is used as reference. For the spatial-averaged ETC properties, ERA5 shows a good skill for wind speed with normalized mean bias (NMB) of −0.7% and normalized root-mean-square error (NRMSE) of 14.3%, despite a tendency to overestimate low winds and underestimate high winds. The ERA5 skill is worse for precipitation than for wind speed with NMB of −10.4% and NRMSE of 56.5% and a strong tendency to underestimate high values. For both variables, the best and worst performance is found in DJF and JJA, respectively. Negative biases are often identified over regions with stronger precipitation/wind speeds, and a systematic underestimation of wind speed is found over the Rockies with complex topography. Compared to the averaged ETCs, ERA5's performance deteriorates for the top 5% extreme ETCs with a stronger tendency to underestimate both wind speed and precipitation (NMB of −10.2% and −22.6%, respectively). Furthermore, ERA5's skill is worse for local extreme values within ETCs than for spatial averages. Our results highlight some important limitations of the ERA5 reanalysis products for studies looking at the possible impacts of ETCs.

KEYWORDS
ERA5 evaluation, extratropical cyclone, local extremes, near-surface winds, precipitation

1 | INTRODUCTION

Extratropical cyclones (ETCs) modulate the weather variability in mid-to-high latitudes and constitute an

Ting-Chen Chen and François Collet should be considered joint first authors.

essential component of the atmospheric general circulation (e.g., Catto et al., 2019). ETCs are favoured over regions with strong low-level temperature gradients (baroclinic instability), but orographic effects (e.g., lee cyclogenesis) and diabatic effects (e.g., surface fluxes, latent heating) are also important contributing factors for cyclone development (Hoskins, 1990; Petterssen & Smebye, 1971; Uccellini, 1990). In regions dominated by their occurrence, ETCs are often the main contributor to local extreme precipitation and near-surface wind, shaping the regional climatology and causing severe damages (Booth et al., 2015; Hawcroft et al., 2012; Kunkel et al., 2012). For example, the Halloween storm in 2019 swept through eastern Canada with heavy precipitation and damaging wind gusts, resulting in over 250 million in insured damages and the most severe power outage in Quebec province in 20 years (Government of Canada, 2020; Insurance Bureau of Canada, 2019). Therefore, improving our ability to capture and understand ETCs' space–time features and impacts is of great social-economic and climatic importance.

To characterize the lifecycle of ETCs, including their frequency and intensity, reanalysis data are generally used due to their homogeneous availability in time and space, especially over oceans where ETCs are active but in-situ observations are sparse (e.g., Di Luca et al., 2015; Hodges et al., 2011; Rudeva & Gulev, 2011; Simmonds & Keay, 2000; Wang et al., 2006). To obtain a climatology of ETCs, Lagrangian approaches employ objective identification and tracking algorithms, usually using mean sea level pressure or relative vorticity fields (e.g., Neu et al., 2013). Statistical cyclone properties can then be constructed, and the storm structure can be obtained via cyclone-centered composites of temperature, low-level wind speed, precipitation, and so forth (e.g., Bauer & Del Genio, 2006; Booth et al., 2018; Field & Wood, 2007; Pepler et al., 2018; Sinclair et al., 2020). Some climate-model-based studies assess the response of ETCs to climate change by comparing the cyclone statistics over a historical period with those simulated under projected future climate scenarios. In such studies, reanalysis data are still important as they are often taken as a baseline to evaluate the performance of climate models via hindcast simulations (e.g., Catto et al., 2010; Feser et al., 2015; Zappa et al., 2013). Additionally, reanalysis products are also frequently used to assess the precipitation, wind, and/or compound extremes brought by ETCs (e.g., Hénin et al., 2021; Owen et al., 2021).

However, a reanalysis is only a proxy of the actual atmospheric conditions, and different reanalysis datasets do not necessarily agree with each other in the representation of ETCs due to the varying model physics, resolution, observations being ingested, and assimilation techniques (e.g., Naud et al., 2018; Wang et al., 2016). While intercomparison studies indicate that recent reanalysis products show converging results in terms of the number and location of ETCs (e.g., Catto et al., 2010; Di Luca et al., 2015; Hodges et al., 2011), large uncertainties are still found in the instantaneous fields at small spatial scales (Hodges et al., 2011), particularly for weak cyclones (Neu et al., 2013). Furthermore, it has been shown that reanalysis contains more significant biases in extreme than non-extreme weather conditions (e.g., Campos et al., 2022; Lei et al., 2022). For example, Campos et al. (2022) evaluated the quality of near-surface winds in the ERA5 reanalysis using higher spatiotemporal resolution satellite data over the Atlantic Ocean. They found greater discrepancies (with ERA5 underestimating winds by approximately 10%–15%) with the presence of tropical or ETCs than no-cyclone conditions. They also showed that the relative underestimation of ERA5 increases as the winds become more extreme.

While many studies have assessed the quality of reanalysis products for different variables with various reference data, most of them either considered a fixed geographical region without differentiating ETC events (e.g., Jiao et al., 2021; Minola et al., 2020; Molina et al., 2021; Peña-Arancibia et al., 2013) or focused on oceanic cyclones only (e.g., Naud et al., 2018, 2020; Pepler et al., 2018). Although reanalysis assimilate relatively more observational data over land than ocean, the complex terrain and heterogeneous land types may pose greater challenges for models and reanalysis products to represent the near-surface atmospheric variables that are strongly dependent on local characteristics (e.g., Brune et al., 2021; Gualtieri, 2022; Jiménez et al., 2008; Lavers et al., 2022; Minola et al., 2020). It is therefore important to investigate the reliability of reanalysis for ETCs over the continent, where human activities are directly affected.

Therefore, this study aims to address this gap by evaluating the skill of the most up-to-date and widely-used global reanalysis product from the European Centre for Medium-Range Weather Forecasts (ECMWF), the ERA5 reanalysis (Hersbach et al., 2020), at representing 10-m wind speed and precipitation associated with ETCs over North America during 2005–2019. We utilize the in-situ station data from the Integrated Surface Database (ISD) as the reference, considering that the near-surface wind and surface precipitation observations from ISD are not directly assimilated in ERA5. We identify and track ETCs with an objective algorithm and, using the centre of each cyclone and a constant radius, we perform the evaluation of ERA5 using two quantities: a spatial average and a spatial extreme over

each cyclone. The first quantity provides an assessment of the actual quality of the ERA5 reanalysis. The second measure evaluates not only the ERA5 quality but also the distinct spatial representativity of station and ERA5 data (Lavers et al., 2022). All analyses are made at the seasonal and annual scale. Section 2 describes the datasets, the methodology for cyclone tracking and data processing, and the evaluation metrics. Results are shown in Section 3. Section 4 discusses the sensitivity of our results to various methodological choices, and a comparison between our main findings with previous studies. Conclusions are presented in Section 5.

2 | DATA AND METHODS

2.1 | The ERA5 reanalysis

ERA5 is the latest reanalysis produced by the ECMWF and provides a range of atmospheric, land-surface and sea-state variables over the globe (Hersbach et al., 2020). ERA5 is based on the Integral Forecasting System (IFS) Cycle 41r2 model, which has a horizontal resolution of 31 km and uses a total of 137 levels in the vertical (the model's top is at 0.01 hPa). The model also uses a state-of-the-art representation of sub-grid scale processes, including a scheme for large-scale cloud and precipitation with prognostic variables for precipitating rain and snow and a revised deep-convection scheme (see Hersbach et al., 2020 and references therein). In the surface layer (up to the lowest model level at about 10 m), the model uses Monin–Obukhov similarity theory to represent turbulent fluxes between the surface and the atmosphere. The model also uses a parametrization of orographic drag that will affect near-surface wind speeds (ECMWF, 2016).

In this study, the ERA5 reanalysis data, available hourly on a regular latitude–longitude grid with a grid spacing of 0.25°, are used with a double objective. First, we use its mean sea level pressure and 850-hPa relative vorticity fields to identify and track ETCs over North America (see Section 2.3). Second, total surface precipitation and 10-m wind speed are used to assess the ability of the reanalysis to reproduce high-impact variables associated with ETCs. Total precipitation represents the accumulated liquid and frozen water that falls over a grid box during each hour and corresponds to the sum of convective precipitation calculated by the convection parametrization and the large-scale precipitation. Although surface precipitation observations are not directly assimilated, the ERA5 assimilates the NCEP stage IV precipitation estimates (Lin & Mitchell, 2005) that combine NEXRAD precipitation estimates with gauge measurements (Hersbach et al., 2020). NCEP stage IV is only available in the United States. The 10-m wind speed is derived from the instantaneous zonal (u) and meridional (v) wind speed components at 10 m height ($ws=\sqrt{u^2+v^2}$). The ERA5 10-m wind speed is a diagnosed product to be compatible with the wind observations from SYNOP (surface SYNOPtic observations) stations. Because the station requires wind measurement to be in open terrain, an exposure adjustment is included in ERA5 10-m winds (ECMWF, 2016).

Because ground-based observation instruments have a finite detectable precision but ERA5 does not, ERA5 likely has a positive bias against ISD at the low end of the wind/precipitation distributions. To take this precision issue into account, we adjust the ERA5 grid-point value to 0 if the wind speed is smaller than 0.5 m/s and if the precipitation rate is smaller than 0.2 mm/h, based on some up-to-date instruments manuals for rain gauges and wind sensors (Vaisala, 2020, 2021). Note that these thresholds also seem reasonable based on our examination on the station data utilized in this study: For wind speed, most stations have a minimum non-zero values of either ∼0.1, 0.5 or 1.5 m/s, while for precipitation, the majority show a value of ∼0.2 mm/h (Figure S1).

2.2 | The ISD

The ISD developed by the National Centers for Environmental Information (NCEI) at the National Oceanic and Atmospheric Administration (NOAA) archives sub-daily observations from more than 20,000 automated and manual surface weather stations across the globe (NOAA-NCEI, 2018; Smith et al., 2011). It includes multiple sources of meteorological reports and comprises several atmospheric variables, including surface precipitation, 10-m wind speed and direction, 2-m air and dew point temperature, atmospheric sea level pressure and more. This study uses 10-m wind speed and precipitation variables recorded in North America (10 N–75 N and 120 W–40 W region) during 2005–2019. The precipitation variable ("AA1 in the ISD dataset") includes rain, snow and any other frozen precipitation, melted down into a water-equivalent value by Automated Surface Observing System stations with heated bucket rain gauges (NOAA, 1998). In order to merge multiple types of reports into one dataset, ISD included a series of quality checks, assessing the data validity, consistency between variables, temporal continuity, and so forth. Based on these checks, each observed variable is flagged with a quality code and expressed in a uniform format (NOAA-NCEI, 2018). Readers are referred to Lott (2004) for more information.

In this study, we employ additional ISD data selections and post-processing techniques to compare with ERA5. The first selection is based on the type of data report. Several weather stations that transmit hourly METAR (METeorological Aerodrome Reports) also transmit intermediate METAR/SPECIs (METAR SPECIal reports) every 20 min. Even though intermediate reports were recorded as 1-h accumulations, our manual checks suggest that the precipitation in these reports was accumulated for less than 1 h, likely due to the constraints of the ISD data format. Therefore, we leave out the METAR/SPECIEs and AUTO (METAR reported without human supervision) reports for precipitation data. For wind speed observations, we exclude the NOAA's Climate Reference Network data because they are primarily hourly averages and thus not compatible with the instantaneous winds we use from ERA5. To sum up, we consider METAR and the NOAA's Climate Reference Network data for precipitation and METAR, METAR/SPECIs, AUTO, SAO (Surface Airways Observation) and SYNOP for wind speed.

Next, we filter data based on their quality code and observational type. Precipitation and wind speed observations that do not pass all ISD quality checks (i.e., quality code different than 1 or 5, which indicates 'passed all quality control checks' and 'passed all quality control checks, data originate from an NCEI data source', respectively; NOAA-NCEI, 2018) are discarded. For precipitation, only the 1-h accumulated records are considered (i.e., accumulation period code of 1). For wind speed, the type codes that indicate 5-, 60- and 180-min averaged wind speed are removed. To our knowledge, the remaining wind speed observations represent the 2-min averages at 10 m above the ground surface (Environnement et Changement Climatique Canada, 2021; NOAA-NCEI, 2018).

Because not all observations are recorded at the exact hour, to compare them with the hourly ERA5 data, we select the nearest-to-the-hour ISD observations within a specified time window. The nearest 1-h accumulated precipitation report that passes all ISD quality checks within 15 min prior to each hour is utilized, no matter whether the accumulated value is zero or not, while the wind observation within a 30-min window centred on each hour is selected. If several weather reports are recorded at the same time for the same station, only the first

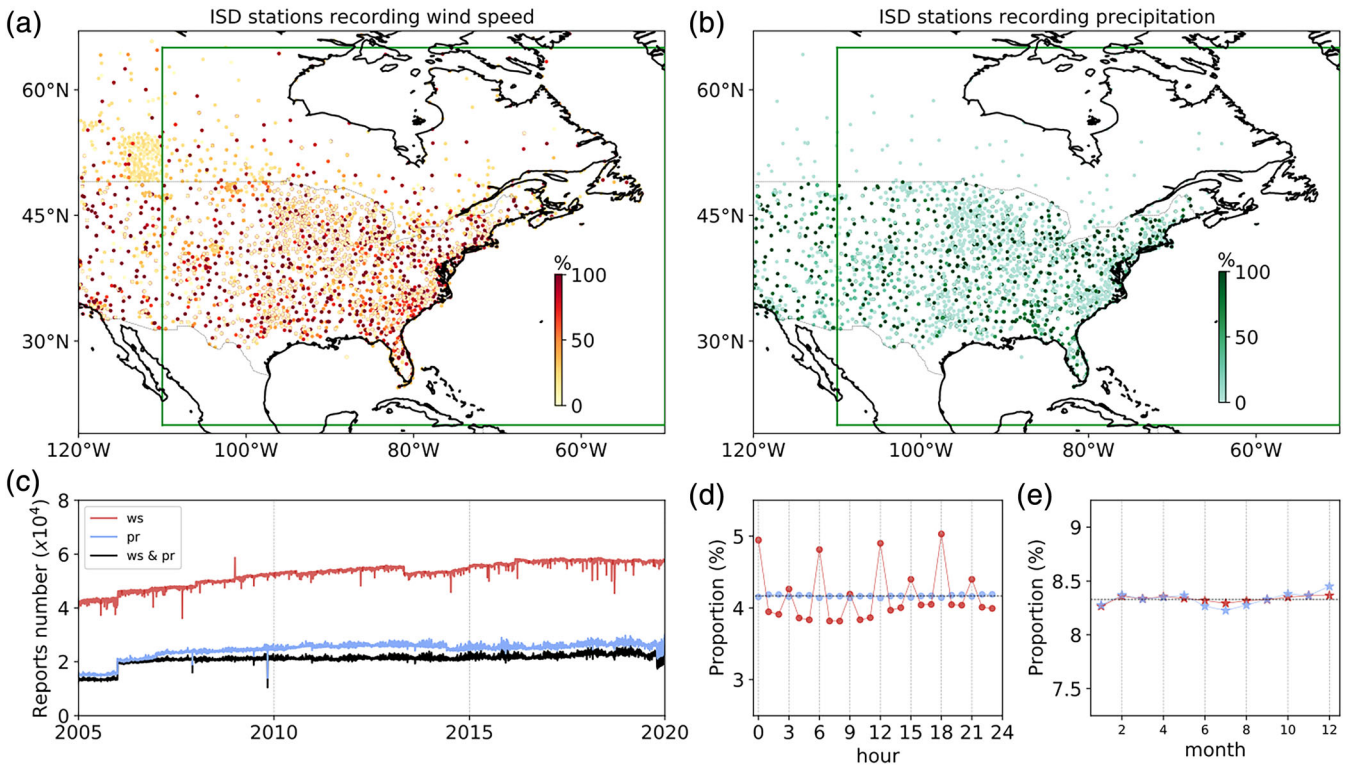

FIGURE 1 (a) The location of integrated surface database (ISD) stations for wind speed observations used in this study. The colours indicate the proportion of such data available for the entire 2005–2019 period. The green frame represents the region used to select cyclones, as described in Section 2.3. (b) Same as (a) but for precipitation. (c) Total number of reports per day for wind speed, precipitation and both (simultaneously) as a function of time. (d) The proportion of wind speed (red) and precipitation (blue) observation as a function of the UTC hour of the day. (e) Same as (d) but of the month of the year, with proportion standardized to a month of 30 days. [Colour figure can be viewed at wileyonlinelibrary.com]

report is utilized. We note that the cumulative distributions of these two observational variables are not continuous as many records have a discrete unit/increment of one knot (i.e., 0.51 m/s) for wind speed and 0.01 inch (i.e., 0.254 mm/h) for precipitation.

The above ISD data processing leads to a total of 3831 and 2809 stations used at least once for wind speed and precipitation, respectively (Figure 1a,b). These stations are not homogeneously distributed over North America, with a higher density in the central and eastern United States and a lower (zero) density in Canada (Mexico). There are almost doubled amounts of wind speed reports compared to precipitation reports, but none of them show sharp changes during our study period (Figure 1c), nor do they show large variation across the hour of the day or the month of the year (Figure 1d,e). The temporal availability of stations differs with variables. For all 3831 stations reporting wind speed, about 47% of them have hourly data for more than 50% of the 2005–2019 period, while 32% of the stations have data for more than 90% of the period. For precipitation, around 31% and 24% of the 2809 stations have hourly observations covering more than 50% and 90% of the period of interest, respectively. While these values may seem low, they are somewhat underestimated measures of the station data's actual completeness for multiple reasons. First, they only account for the selected data after the above filtering. Second, more than 300 stations only provide SYNOP reports that are not provided hourly, and about 1400 stations provide at least one SYNOP report. Finally, about 50% of the stations used in this study have an operating length shorter than the study period. Since this work does not involve any trend analysis, we do not put an additional selection criterion based on the stations' temporal coverage. Nevertheless, we have conducted an examination based on a longer study period from 2000 to 2019 with an even lower percentage of temporal coverage and found consistent results (not shown).

Finally, the selected ISD data are spatially interpolated to the ERA5 $0.25 \times 0.25^{\circ}$ latitude–longitude regular grid over North America. For each ERA5 grid cell, we consider the available ISD observation that is located within and nearest to the centre of the grid cell. If ISD data are not available, a missing value is recorded. We have also tested an averaging method, for which the average of all ISD observations within one grid cell is taken, but the results do not change significantly from the nearest-station method due to the sparse ISD station density with respect to the ERA5 grid resolution. As shown in Figure S2, only a small number of ERA5 grid cells contain multiple ISD observations.

2.3 | ETC tracks

ETC tracks are obtained by applying a cyclone tracking algorithm developed at the University of Quebec at Montréal with the hourly ERA5 data (Chartrand & Pausata, 2020; Chen et al., 2022). This algorithm identifies cyclone centres based on the mean sea level pressure and the 850-hPa relative vorticity. For this study, we only consider ETCs whose centres remain in central and eastern North America (continental regions within 110–50 W and 20–65 N; named CENA hereafter) for more than 24 h. The western part of North America is not included because the tracking algorithm is unreliable over regions with high topography. It should be noted that some of the cyclones identified might be tropical cyclones and tropical transitions as no additional filter is applied to only select ETCs. A total of 3643 cyclone tracks/cases are identified, resulting in a total of 310,000 hourly records of 'cyclone centre'.

2.4 | ETC-associated 10-m wind speed and precipitation

To evaluate ERA5 for ETC events, we compare the wind speed and precipitation variables against observations, when and where applicable within a 1000-km radius of a cyclone centre. This horizontal length is assumed to be suitable to capture the bulk impacts and the embedded local extremes associated with ETCs (e.g., Catto et al., 2010; Field & Wood, 2007; Jeyaratnam et al., 2020). Results based on a smaller radius of 500 km are discussed in Section 4.1.

To ensure a fair comparison, three additional criteria are imposed. First, while there can be as many as 7500 ERA5 grid cells within a 1000-km-radius circular region, only a few hundred ISD observations are available in most cases. To account for the spatial heterogeneity of ISD stations, ERA5 grid points are masked out where and when no interpolated ISD observation is available. Second, because ISD stations are mostly over land but can be on the shore, we discard all ERA5 grid points for which the land-sea mask is lower than 0.5, a suggested minimum value indicating a mixture of land and inland water but not ocean (Copernicus Climate Change Service, Climate Data Store, 2023). The second criterion is required because some coastal or lakeside ISD stations can be interpolated to an almost pure-water ERA5 grid point. Note that we have also tested a lower land-sea mask threshold of 0.2, including grid points with a higher ocean/lake fraction, and found a larger difference between ERA5 and ISD, a natural bias due to the different surface roughness lengths between land and water/ice. Third, only the cyclone centres with at least 100 interpolated ISD

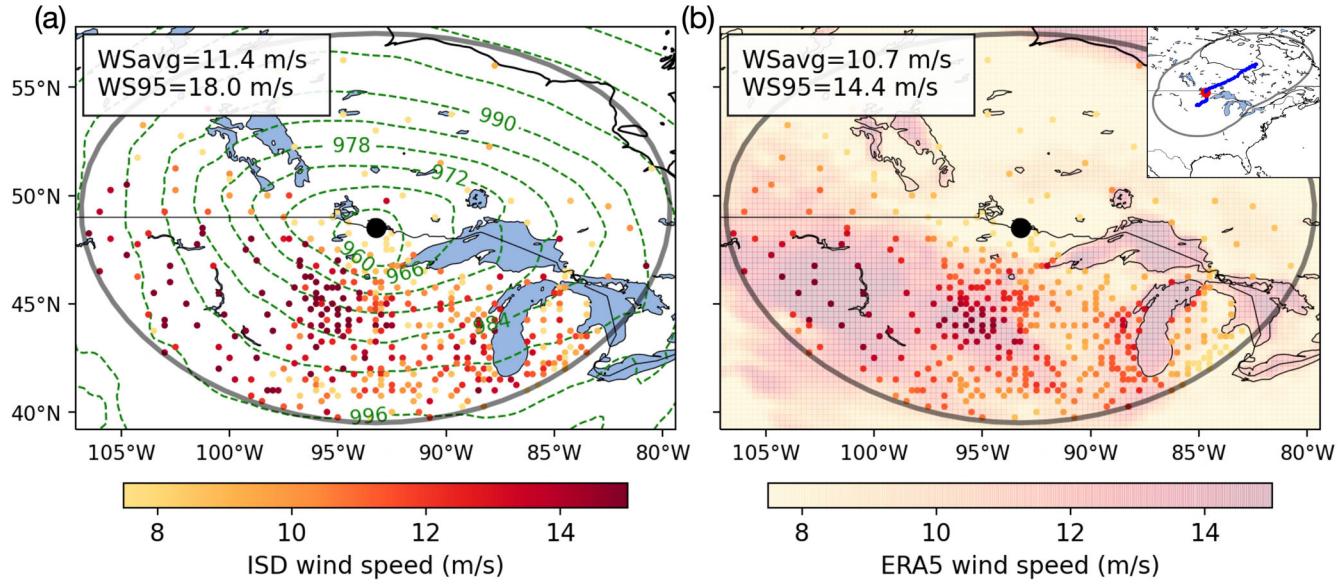

FIGURE 2 (a) An example showing the identification of WSavg and WS95 for a given cyclone centre at 48.5°N, 93.25°W, at 2100 UTC on 26 October 2010, overlaid with the ERA5 mean sea level pressure (green dashed contours; hPa). The grey solid circle represents the cyclone's 1000-km domain, which includes 313 ISD stations in this case (small dots; wind speed shown in colours), from which the WSavg and WS95 are derived (upper-left box). (b) The ERA5 10-m wind speed for the same cyclone centre, with the complete native field shown in translucent shadings and the unmasked ERA5 grid values (to be compared with ISD) shown in small dots as in (a). The whole track of this cyclone is shown in the upper-right corner. ISD, Integrated Surface Database. [Colour figure can be viewed at wileyonlinelibrary.com]

observations within the 1000-km radius were considered. This threshold was arbitrarily set by a trade-off between having sufficiently large observational samples for each cyclone and having enough cyclones to systematically examine the potential bias for ETCs. Our results do not change substantially when different thresholds of 50, 100 and 200 stations are used (Figure S3).

To evaluate ERA5's skill in representing ETCs' overall impacts, the spatial averages of all unmasked ERA5 and ISD grid-point wind speed and precipitation, named WSavg and PRavg, respectively, are computed for each cyclone centre. An illustration example is given in Figure 2. Since only the unmasked data are considered, it should be borne in mind that WSavg and PRavg do not present realistic cyclone statistics and are biased towards regions with high density of observations (Chen et al., 2022). In addition, to assess ERA5's performance in capturing the extremes, we further examine the most extreme cyclone centres based on the top 5% of WSavg/PRavg and the local extremes within the cyclones based on the spatial 95th, 98th and 99th percentiles in each 1000-km cyclone domain. For the latter, we will focus on results based on the 95th percentiles (noted as WS95 and PR95 for wind speed and precipitation, respectively) and the sensitivity to different percentiles will be shown in Section 4. Note that in the evaluation for spatial extremes, we do not require ERA5 and ISD to capture them at the same grid points. Instead, we are interested in whether ERA5 can produce similarly strong magnitudes within ETCs.

2.5 | Evaluation metrics

To assess the ERA5 performance, we use several quantitative metrics, including the bias, root mean squared error (RMSE), Pearson correlation coefficient and ordinary least squares regression analysis. To investigate the seasonal skill, these metrics are also calculated for cyclones in different seasons.

First, the normalized mean bias (NMB) is calculated as the averaged difference (bias) for a target variable C between ERA5 and ISD across all cyclones, normalized by the mean value of the observation:

$$\mathrm{NMB} = \frac{\mathrm{bias}}{\overline{C^{ISD}}} = \frac{\frac{1}{n}\sum_{i=1}^{n}\left(C_i^{ERA5} - C_i^{ISD}\right)}{\frac{1}{n}\sum_{i=1}^{n} C_i^{ISD}} \quad (1)$$

where C_i denotes WSavg_i, PRavg_i, $\mathrm{WS95}_i$ or $\mathrm{PR95}_i$ for the cyclone centre i, and the overbar denotes the averages over n cyclone centres. Defined this way, NMB gives more weight to ETC tracks that last longer and facilitates the comparison of errors across different variables, seasons and regions, taking into account the varying background intensity.

Similarly, the normalized root-mean-square error (NRMSE) measures the RMSE between ERA5 and ISD scaled by the averaged ISD observational value:

$$\mathrm{NRMSE} = \frac{\mathrm{RMSE}}{\overline{C^{ISD}}} = \frac{\sqrt{\frac{1}{n}\sum_{i=1}^{n}\left(C_i^{ERA5} - C_i^{ISD}\right)^2}}{\frac{1}{n}\sum_{i=1}^{n} C_i^{ISD}}. \quad (2)$$

Finally, the Pearson correlation coefficient (CC) is used to measure the linear association between the variables derived from ERA5 and ISD:

$$\mathrm{CC} = \frac{\sum_{i=1}^{n}\left(C_i^{ERA5} - \overline{C^{ERA5}}\right)\left(C_i^{ISD} - \overline{C^{ISD}}\right)}{\sqrt{\sum_{i=1}^{n}\left(C_i^{ERA5} - \overline{C^{ERA5}}\right)^2}\sqrt{\sum_{i=1}^{n}\left(C_i^{ISD} - \overline{C^{ISD}}\right)^2}}. \quad (3)$$

3 | RESULTS

3.1 | Cyclone distribution for WS and PR evaluation

Figure 3 shows the total number of cyclone centres that occurred in each ERA5 grid cell over the CENA region during 2005–2019. Note that this is not the climatology of all cyclones but only those qualified for our evaluation. That said, large densities of cyclone centres still agree with the well-identified cyclone-active regions: the lee side of the Rockies where frequent cyclogenesis occurs, the Great Lakes region where enhanced heat fluxes foster cyclone development/steepening and where cyclone tracks of Alberta Clippers and Colorado Lows converge, and the eastern coastline upstream to the Gulf Stream where storm track prevails (e.g., Plante et al., 2015; Poan et al., 2018; Reitan, 1974). The different sample sizes between the two variables are caused by the availability of observation records (Section 2.4), and wind speed observations are globally more numerous than precipitation observations (Figure 1a,b). Out of the total number of cyclone centres identified by the tracking algorithm, about 30% and 21% are retained for wind speed and precipitation variables, respectively. The number of cyclone centres varies with seasons, with the smallest number in JJA (with 21,258 and 12,198 cyclone centres for wind and precipitation, respectively) and the largest number in MAM (with 27,586 and 20,314 cyclone centres for wind and precipitation, respectively). Yet, the distribution of cyclone centre density does not change substantially between seasons for both variables (not shown).

3.2 | Evaluation of ETC averages

3.2.1 | Domain averages of WSavg and PRavg

We first assess the ability of ERA5 in representing the ETCs' spatial-mean wind speed. Figure 4a–d show the scatter plots of WSavg between ERA5 and ISD in DJF, MAM, JJA and SON. It is clear that most of the data points are distributed along the 1:1 line, indicating an overall good agreement between ISD and ERA5. The annual averaged WSavg estimated from ISD and ERA5 are very close with the same rounded values of 4.3 m/s (Figure 4e). However, the lower slope of the linear fit compared with the 1:1 line suggests that ERA5 tends to be positively biased at low wind speed values and negatively biased at high values in all seasons. Consistently, the quantile–quantile plots (red diamonds in Figure 4a–d) show that ERA5 and

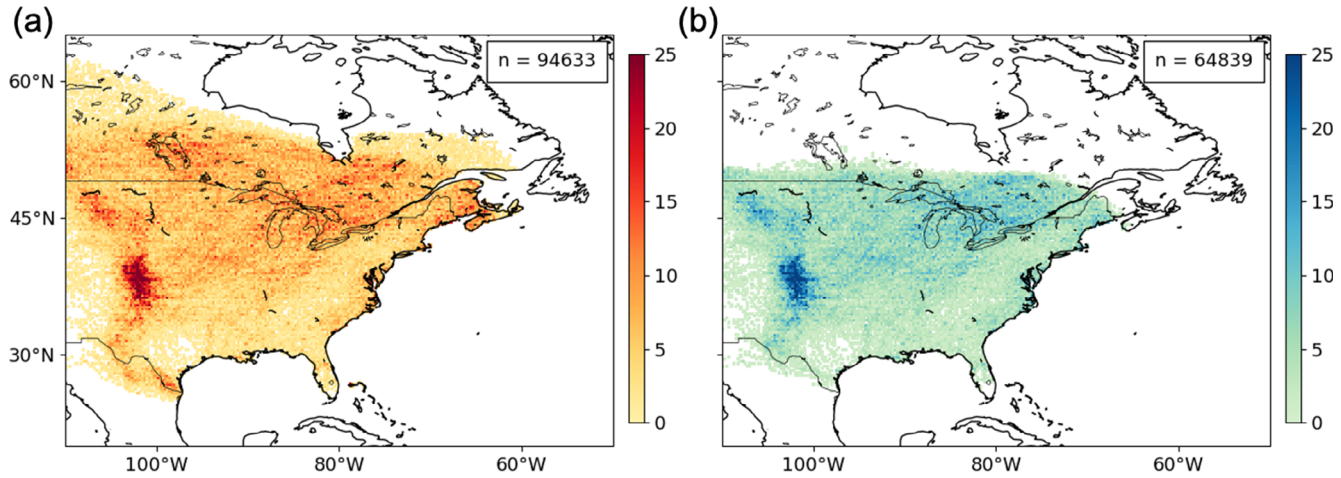

FIGURE 3 (a) Number of cyclone centres at each grid point with more than 100 10-m-wind-speed observations available within their 1000-km radius during 2005–2019 period. The total number of cyclone centres (n) is shown on the top right corner of each map. (b) Same as (a) but for precipitation observations. [Colour figure can be viewed at wileyonlinelibrary.com]

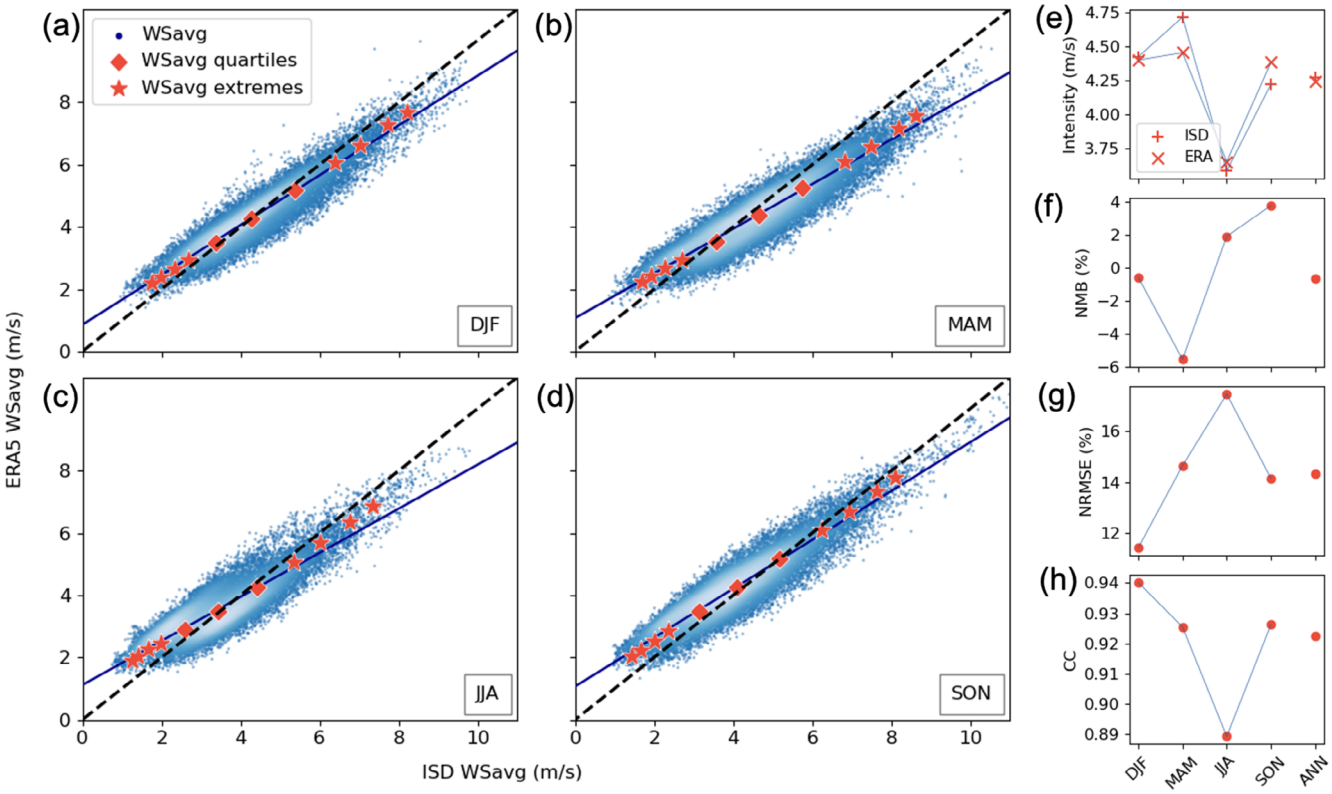

FIGURE 4 (a–d) Seasonal scatter plot of ISD against ERA5 WSavg with Gaussian density in blue shades. Quantile–quantile plots are shown in red diamond markers for 25th, 50th and 75th quantiles and star markers for 1st, 2nd, 5th, 10th, 90th, 95th, 98th and 99th quantiles for each season. The ordinary least squares regression is shown with a blue line in each plot. (e) Averaged WSavg intensity for both ISD and ERA5, (f) NMB, (g) NRMSE and (h) Pearson correlation coefficient (CC), all calculated seasonally and annually over the 2005–2019 period. [Colour figure can be viewed at wileyonlinelibrary.com]

ISD agree quite well in the middle range, whereas the low quantiles of ERA5 (the 1st, 2nd, 5th and 10th) tend to be higher than ISD and the high quantiles of ERA5 (the 90th, 95th, 98th, and 99th) tend to be lower than ISD. The annual normalized mean bias (NMB) is low (−0.7%) although the NRMSE is a bit higher (14.3%). The annual correlation (CC) is 0.92, demonstrating a good linear relationship between ERA5 and ISD. In general, ERA5 well represents the WSavg despite slightly larger deviations for lower and higher values.

On the seasonal scale, most error metrics show the worst performances of ERA5 in JJA when the averaged WSavg reaches the annual minimum at 3.7 m/s (Figure 4e). JJA has the highest NRMSE with a value of 17.5% and the lowest CC of 0.88, indicating a larger spread of ERA5 values (larger uncertainty) corresponding to the same value of ISD. In contrast, ERA5 exhibits the best performance in DJF with NMB close to 0%, NRMSE of 11.4% and CC of 0.94. For both MAM and SON, ERA5 shows intermediate performances with NRMSE values of 14.6% and 14.2%, and correlation coefficients of 0.93. However, it is interesting to note that the NMB in these transition seasons exhibit peaks magnitudes with opposite signs, −5.5% and 3.8% for MAM and SON, respectively. A closer examination of the quantile–quantile plots shows that the upper tail of WSavg distribution is the most underestimated by ERA5 in MAM while the lower quantiles are the most overestimated in SON (Figure 4b,d). For JJA, despite the large NRMSE, the notable positive and negative biases in both tails partially cancel out and thus lead to a NMB closer to zero than during MAM and SON.

To evaluate ERA5's performance in capturing the ETCs' spatial-mean precipitation intensity, Figures 5a–d show scatter plots of PRavg between ERA5 and ISD of all cyclone centres in each season. Contrary to that for WSavg, ERA5 does not exhibit a notable underestimation at low values and the degree of underestimation at high values varies notably with season. ERA5 represents the annually-averaged PRavg fairly well, with a slightly lower value of 0.25 mm/h than the ISD of 0.28 mm/h. However, the larger dispersion in scatter plots in Figure 5a–d than in Figure 4a–d indicates a greater variability and uncertainty in the precipitation field than in 10-m wind speed. Both the annual NMB (−10.4%) and NRMSE

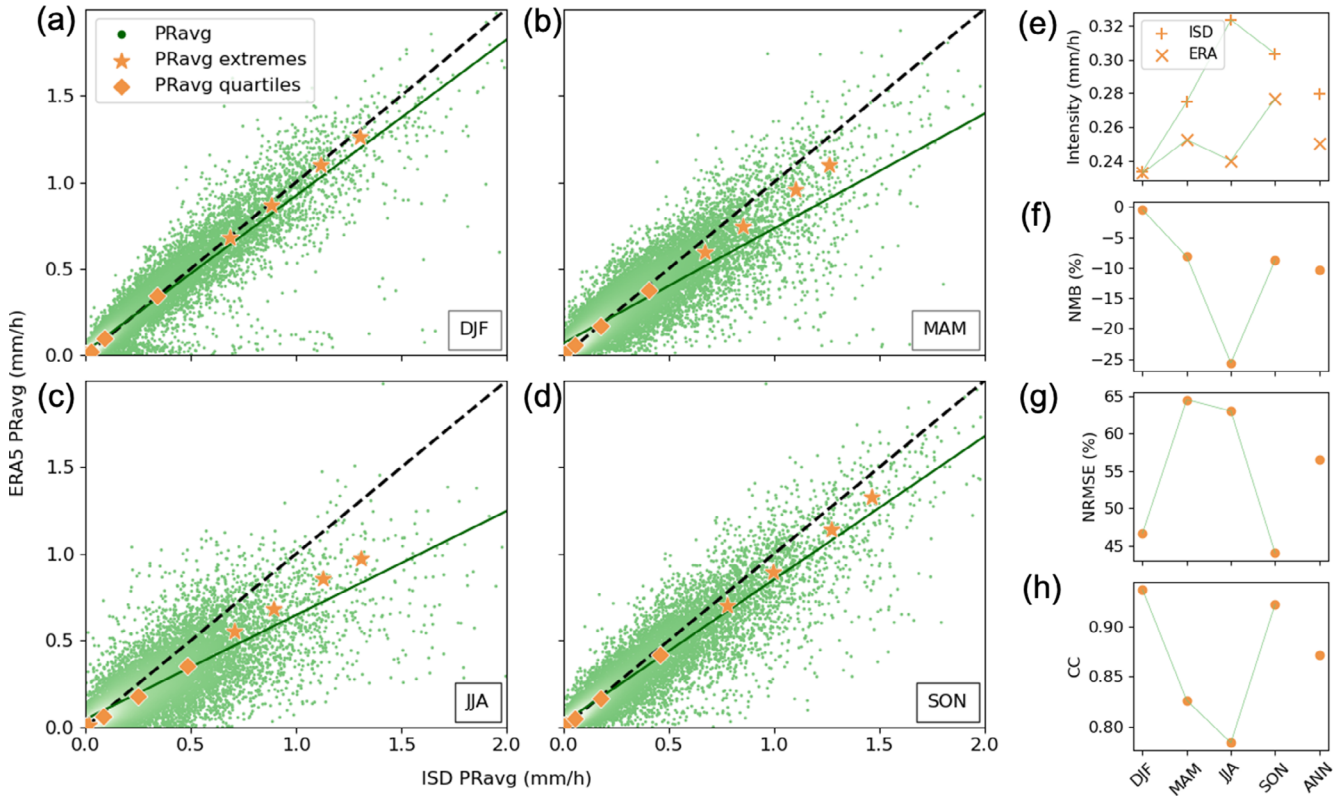

FIGURE 5 Same as Figure 4 but for PRavg. [Colour figure can be viewed at wileyonlinelibrary.com]

(56.5%) for precipitation are at least four times larger than those for wind speed. Consistently, the CC is notably lower (0.87) than for wind speed. Therefore, the quantile–quantile plots (orange markers in Figure 5a–d) can better describe the data than the linear fitted line, showing that the right-skewed precipitation distribution is nevertheless captured reasonably by ERA5 in all seasons except for JJA.

Across seasons, it is clear that the largest disagreement between ISD and ERA5 for ETC precipitation also happens in JJA when the observed value reaches the annual maximum (Figure 5e–h). Such a seasonal PRavg peak in JJA is not captured by ERA5, which shows an annual maximum in SON instead. In JJA, ERA5 severely underestimates the mid and the upper quantiles, leading to the largest magnitudes of NMB (−25.7%), NRMSE (63.0%) and the lowest CC (0.78). This is likely related to the fact that ETCs are more convective in summertime (Jeyaratnam et al., 2020) and that the model resolution is insufficient to resolve the embedded convective processes, which are often accompanied by high-intensity precipitation. In contrast, ERA5 performs relatively better for SON and DJF as the associated quantile distributions are more aligned with the 1:1 line, and their seasonal averaged NRMSE are the lowest (yet still high) at about 45%. Interestingly, NMB is positive only for DJF, indicating a general overestimation of ERA5 in wintertime ETCs' averaged precipitation.

3.2.2 | Spatial variability of WSavg and PRavg

It is of interest to examine whether the above results exhibit some dependency on the geographical feature. We record the observed WSavg value and the associated ERA5-ISD bias at the location of each cyclone centre (see the big central dot in Figure 2) and take the local-grid-cell average of all coinciding centres during 2005–2019 to obtain a spatial distribution (Figure 6). Overall, the intensity of wind speed is higher over/near the Rockies and central United States and lower in the southeastern United States. High wind speeds are also observed in the northeastern CENA, that is, near the entrance to the mid-latitude maritime storm track. The spatial variability of the WSavg bias shows some dependency on the wind intensity: negative biases are observed in regions with stronger WSavg, that is, over the western and northeastern CENA, and positive biases are found mostly over where WSavg are relatively weaker. In addition, Figure 6 suggests a strong tie between bias and the orography. The significant negative bias highlighted over the Rockies in all

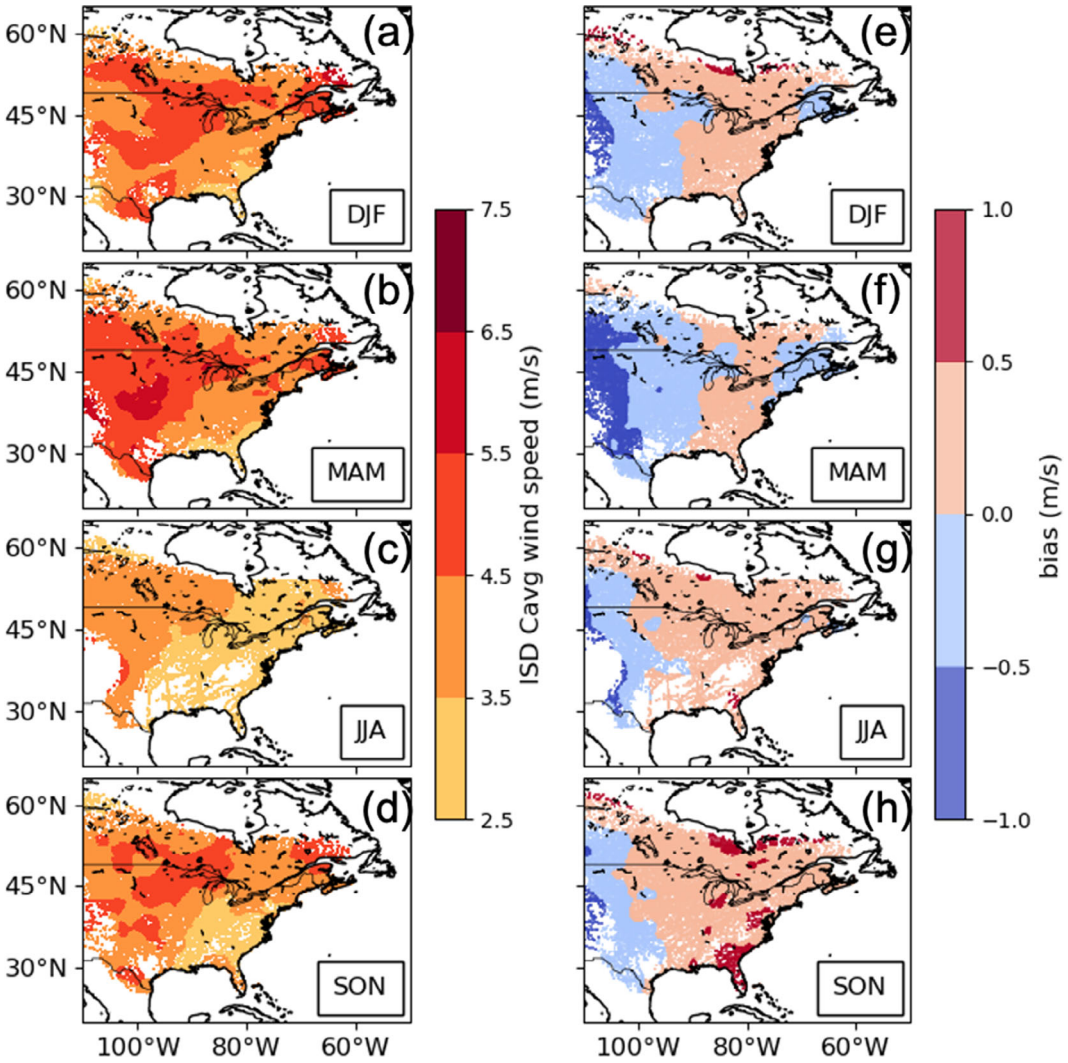

FIGURE 6 Spatial distribution of the ISD WSavg magnitude (left column) and the bias (ERA5-ISD; right column) averaged for all cyclone centers in each season. Note that while WSavg represents the average over a 1000-km domain, the value is recorded only at the grid point of the cyclone centre (the big dot in Figure 2). To improve readability, the raw results have been spatially smoothed via the linear radial basis function interpolation. [Colour figure can be viewed at wileyonlinelibrary.com]

seasons agrees with previous studies that ERA5 tends to underestimate 10-m wind speed in regions with complex topography (e.g., Minola et al., 2020). The underlying reasons include the insufficiently-resolved topographic features and the parametrization of orographic drag in the model (Irina Sandu et al., n.d.). The most negative NMB in MAM (Figure 4f) is associated with the strong winds and thus large negative biases over the Rocky Mountains. On the other hand, the most positive NMB in SON (Figure 4f) corresponds to several patches of positive biases along the east coast, Florida, and near inland lakes, where WSavg seem moderate (Figure 6h).

Figure 7 shows the maps of observed PRavg and bias associated with ETCs. In all, the distribution of PRavg is qualitatively consistent with the climatology of annual precipitation over North America, showing a gradual decrease of precipitation from the Gulf and Atlantic States of the United States towards the Great Plains (e.g., Arsenault et al., 2020; Nelson et al., 2016). Seasonal variations exist in that the relatively wet region extends farther towards the northwestern CENA in MAM, JJA and SON, while it is restricted in the southeastern United States in DJF. Furthermore, in addition to the overall high PRavg near the coast, another peak is observed in the Midwestern United States in JJA (Figure 7c). It has been shown that summertime cyclones exhibit a poleward shift of cyclogenesis and occurrence compared to other seasons (e.g., Reitan, 1974). While summertime ETCs do not produce as strong winds as in other seasons, their contribution to the precipitation is still pronounced. Additionally, Arctic cyclones are active in summer and those track southeastward into the Canadian Arctic Archipelago can transport moisture equatorward to mid-latitude North America (Serreze et al., 2001; Sorteberg & Walsh, 2008). Contrary to the WSavg, the

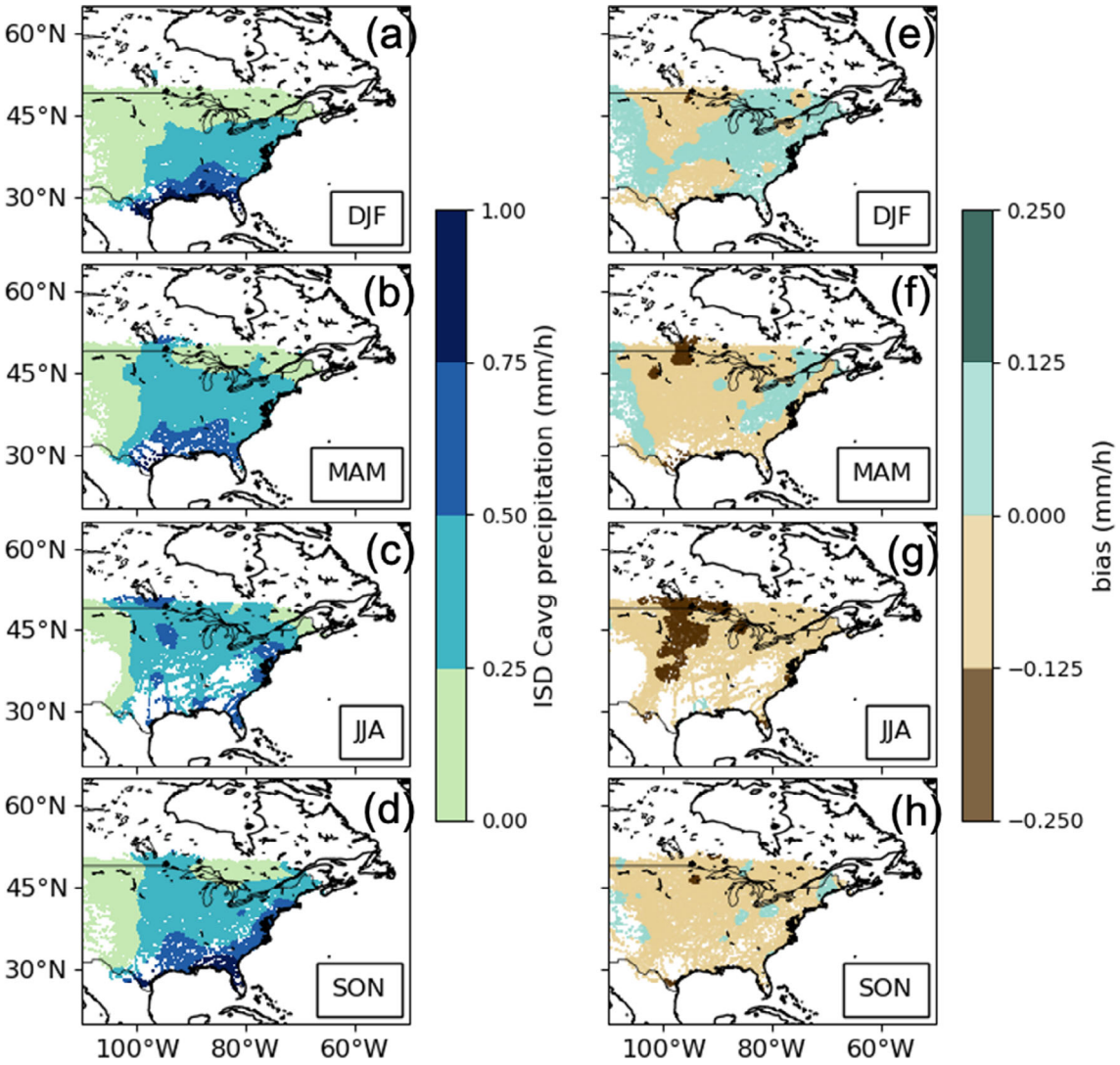

FIGURE 7 Same as Figure 6 but for PRavg. [Colour figure can be viewed at wileyonlinelibrary.com]

PRavg bias does not show a clear dependency on the orography, nor on the distribution of precipitation intensity (Figure 7e–h). DJF exhibits mainly weak positive biases over the entire CENA region, while JJA shows mostly negative biases. Both SON and MAM present weak magnitudes with both signs over CENA. The most negative seasonal bias in JJA (Figure 5f) corresponds to the bias minima of below −0.125 mm/h in Midwestern United States, collocating with the local maxima of PRavg.

3.3 | Evaluation of ETC extremes

3.3.1 | Extreme cases based on WSavg/PRavg

As severe damages are often caused by the rare but extremely strong ETCs, we compare the consistency between the top 5% of WSavg and PRavg as represented in ERA5 and ISD.

For hourly wind speed, the minimum threshold for selecting the top 5% (95th quantile) is 7.0 m/s in ISD and 6.5 m/s in ERA5. Comparing two sets of the top 5%, we find a match of 73%, that is, 3452 out of a total of 4732 observed extreme ETC instances are successfully captured as the top 5% by ERA5. To quantify the intensity difference, we further perform comparisons using two methods. Method 1 compares the intensity of extreme centres by first identifying the top 5% extreme ETC centres in ISD as 'truth' and retrieving these centres from the ERA5 dataset. The derived mean intensity is 7.8 m/s in ISD and 7.0 m/s in ERA5, with an NMB of −10.2%, an NRMSE of 12.5%, and a CC of 0.71. Alternatively, method II compares only the 'matched' ETC instances identified in both ISD and ERA5. The average WSavg is also weaker in ERA5 (7.3 m/s) than in ISD (7.9 m/s), with an NMB of

	Averaged intensity				
	ISD	ERA5	NMB	NRMSE	CC
WSavg	4.3 m/s	4.3 m/s	−0.7%	14.3%	0.92
WSavg top 5%	7.8 m/s	7.0 m/s	−10.2%	12.5%	0.71
WS95	8.5 m/s	7.1 m/s	−17.0%	21.0%	0.92
PRavg	0.28 mm/h	0.25 mm/h	−10.4%	56.5%	0.87
PRavg top 5%	1.18 mm/h	0.92 mm/h	−22.6%	42.6%	0.30
PR95	1.40 mm/h	1.29 mm/h	−7.2%	59.6%	0.87

TABLE 1 Summary of the evaluation of ERA5 against ISD for different quantities.

Note: For the top 5% evaluation, we compare the values of ETC centres identified in ISD (see method I in the text).

Abbreviations: CC, correlation coefficient; ISD, Integrated Surface Database; NMB, normalized mean bias; NRMSE, normalized root-mean-square error.

−7.8%, an NRMSE of 10.0% and a CC of 0.73. In both comparisons, all error metrics except for the NRMSE indicate a worse performance, a systematic underestimation, of ERA5 in capturing the wind speed for extreme cases than for the entire sample (Table 1). The ability of ERA5 in capturing the extreme ETCs decreases with higher quantiles, as the percentage of cyclone matches with ISD is lowered to 63% for the top 1% WSavg cases.

For hourly precipitation, the 95th-quantile thresholds of the PRavg are 0.9 mm/h in ISD and 0.8 mm/h in ERA5. Only 64% of the top 5% PRavg in ISD are successfully captured as the top 5% in ERA5 (i.e., 2068 out of a total of 3242 extreme ETC instances), a lower match rate than for wind speed. Comparison using method I shows a remarkable contrast between ISD and ERA5, with an averaged intensity of 1.18 mm/h in ISD and 0.92 mm/h in ERA5, and the NMB, NRMSE and CC of −22.6%, 42.6% and 0.30, respectively. Comparing only those matched cyclone centres (method II), the averaged intensity is 1.2 mm/h in ISD and 1.1 mm/h in ERA5, and the NMB, NRMSE and CC are −8.6%, 21.0% and 0.66, respectively. Again, except for NRMSE, all error metrics in both comparisons suggest a worse, systematic underestimation of ERA5 in capturing the precipitation intensity for the top 5% than for the entire sample (Table 1). The percentage of matches between ISD and ERA5 is also lowered, from 64% to 54% when we consider the top 1% PRavg instead of the top 5%.

The above results show that ERA5 has a lower skill in capturing the upper tails of wind speed and precipitation averages of all ETC centres, and this is not simply an issue of spatial resolution as the comparisons are all based on the 1000-km-radius averages.

3.3.2 | Local extremes (WS95/PR95)

Finally, we evaluate the performance of ERA5 in capturing the local extreme values, that is, the spatial 95th percentile of hourly wind speed/precipitation (WS95/PR95) within each cyclone centre. For this comparison, some discrepancy is expected given the inherent scale disparity between ERA5 and ISD, because ERA5 variables represent the areal-mean values over a grid cells of about 31×31 km (Chen & Knutson, 2008; Di Luca et al., 2020), while station-based observations are point estimates that account for an area of only a few square km (Chu et al., 2021). Our goal is not to isolate the representativeness of ERA5 but to assess its overall (in)adequacy in applications of extreme analysis and risk assessment at local scales.

For WS95, the annual-mean magnitude is 7.1 and 8.5 m/s for ERA5 and ISD, respectively, that is, almost two times larger than their intensity of WSavg (Figure 8). Compared to the WSavg analysis for the entire and the top 5% samples, ERA5 exhibits a more severe tendency to underestimate WS95 that persists across seasons. Both NMB and NRMSE for WS95 indicate greater errors with annual values of −17.0% and 21.0%, respectively (Table 1). The annual CC of 0.92 is similar to that for WSavg, indicating that the variability across cyclone centres is still well reproduced despite a systematic underestimation. Different from that for WSavg, ERA5 shows its best performance in SON and its worst in MAM for WS95 in terms of NMB and NRMSE, but the lowest seasonal CC is still found in JJA. The spatial variability of the WS95 bias is similar to that of WSavg but is mostly negative with a larger magnitude (Figure S4). In all, the results indicate that ERA5 performs worse in capturing the local extreme values than the overall impacts of averaged/extreme cyclones.

For PR95, the annual-mean magnitude is 1.29 m/s and 1.40 m/s for ERA5 and ISD, respectively, approximately five times as large as the PRavg values on the annual scale (Figure 9). Unlike for the wind speed, the performance of ERA5 is not particularly worse for PR95 than for PRavg with a smaller magnitude of NMB

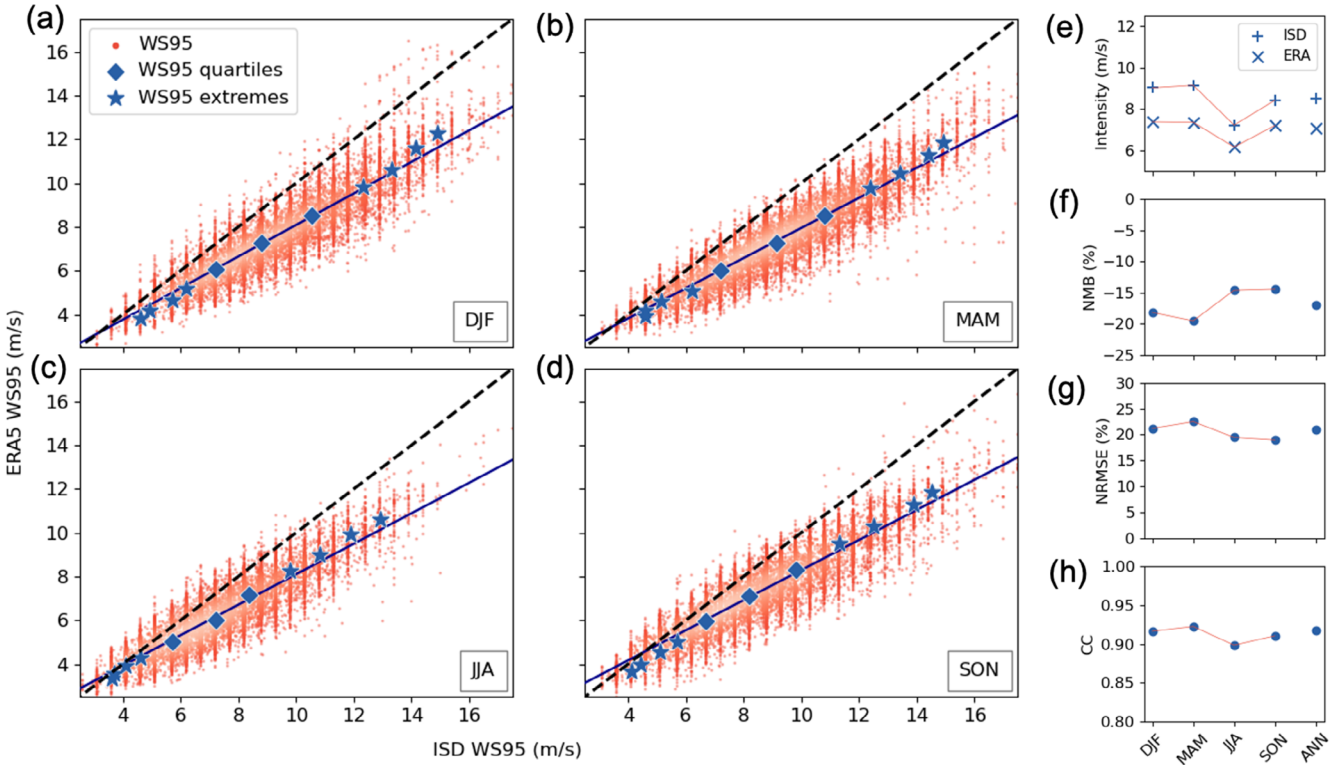

FIGURE 8 Same as Figure 4 but for WS95. [Colour figure can be viewed at wileyonlinelibrary.com]

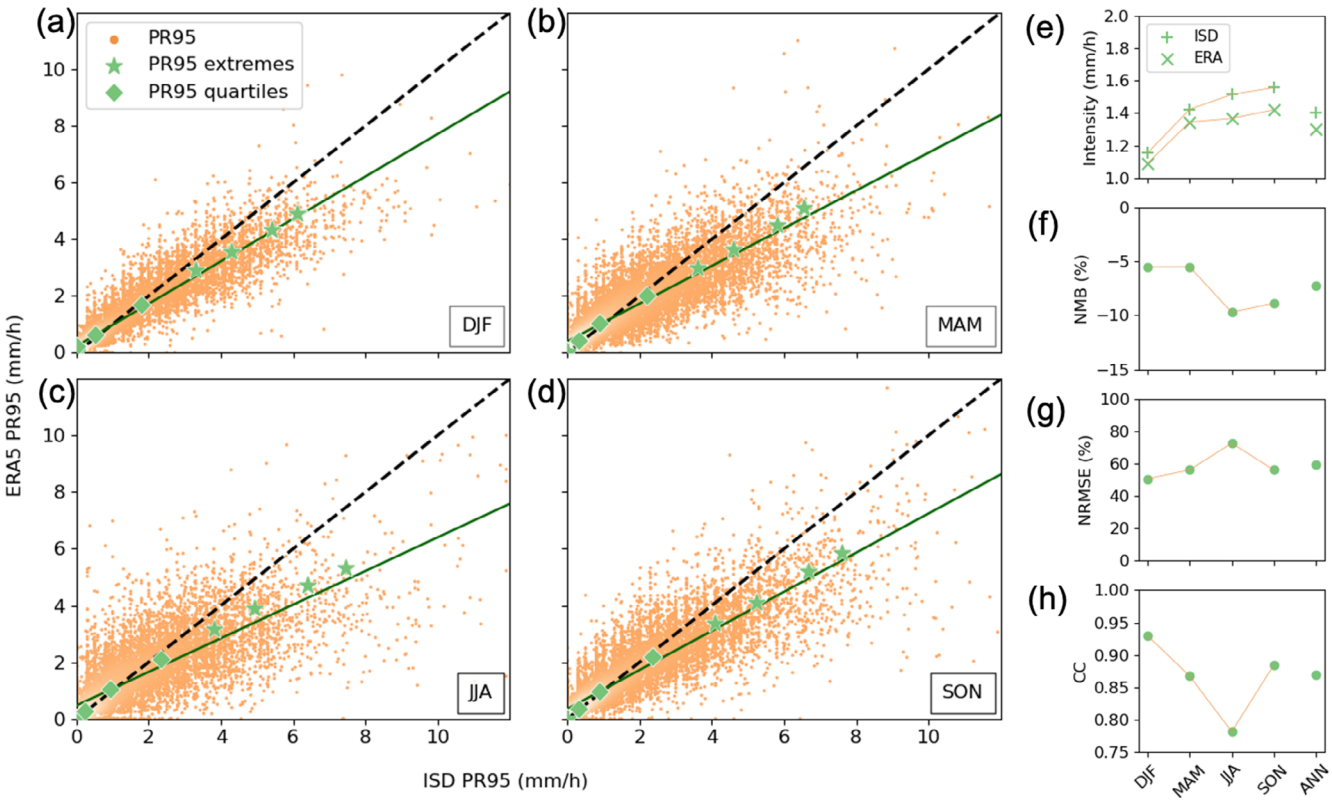

FIGURE 9 Same as Figure 5 but for PR95. [Colour figure can be viewed at wileyonlinelibrary.com]

(−7.2%), a similar CC (0.87) and a slightly higher NRMSE of 59.6% annually (Table 1). The seasonal variation for PR95 remains similar to that for PRavg in that ERA5 still presents the best performance in DJF and the worst performances in JJA. However, two changes are observed. First, the tendency of ERA5 underestimating the upper quantiles becomes notable in all seasons, including DJF (Figure 9a–d). Second, the severe underestimation in JJA in PRavg is improved notably for PR95 in relative terms (Figures 5e,f vs. 9e,f), thus leading to an overall reduced magnitude of NMB. As will be seen in Section 4.2, these results are somewhat sensitive to the chosen spatial percentile for the definition of local extremes. Interestingly, while there is no clear spatial correlation between bias and precipitation magnitude for PRavg, such correspondence emerges for extreme values; larger negative bias tends to occur in regions with higher PR95 and vice versa (Figure S5).

4 | DISCUSSION

4.1 | Sensitivity of results to the cyclone radius

In this study, we examine the sensitivity of our evaluation to the choice of a 500-km radius around ETC centres (Figure S6). Since a smaller radius concentrates on the near cyclone-core region where precipitation and winds are overall stronger, the averaged magnitudes of WSavg and PRavg both increase, with a more notable change in the latter than in the former. While the increase is seen in both ERA5 and ISD, some changes in the error metrics are observed. For wind speed, all error metrics indicate that ERA5 performs slightly worse for the more confined (500-km radius) region than for the larger (1000-km radius) domain surrounding a cyclone, but the seasonal variation remains similar. Such performance degradation is not surprising, as one would expect that as the radius increases, the compensation among local errors will also increase. Furthermore, a larger radius also allows some room for potential shift/dislocation of moderate/strong winds in ERA5. For precipitation, the skill degradation for a smaller calculation radius still holds true in general (except for NMB), but the most severe degradation is observed in MAM, leading to a shift in the worst seasonal performance for PRavg from JJA to MAM.

4.2 | Sensitivity of errors to the definition of local extremes

In this study, we examine the sensitivity of error metrics to the definition of local wind speed and precipitation extremes by considering different spatial percentiles

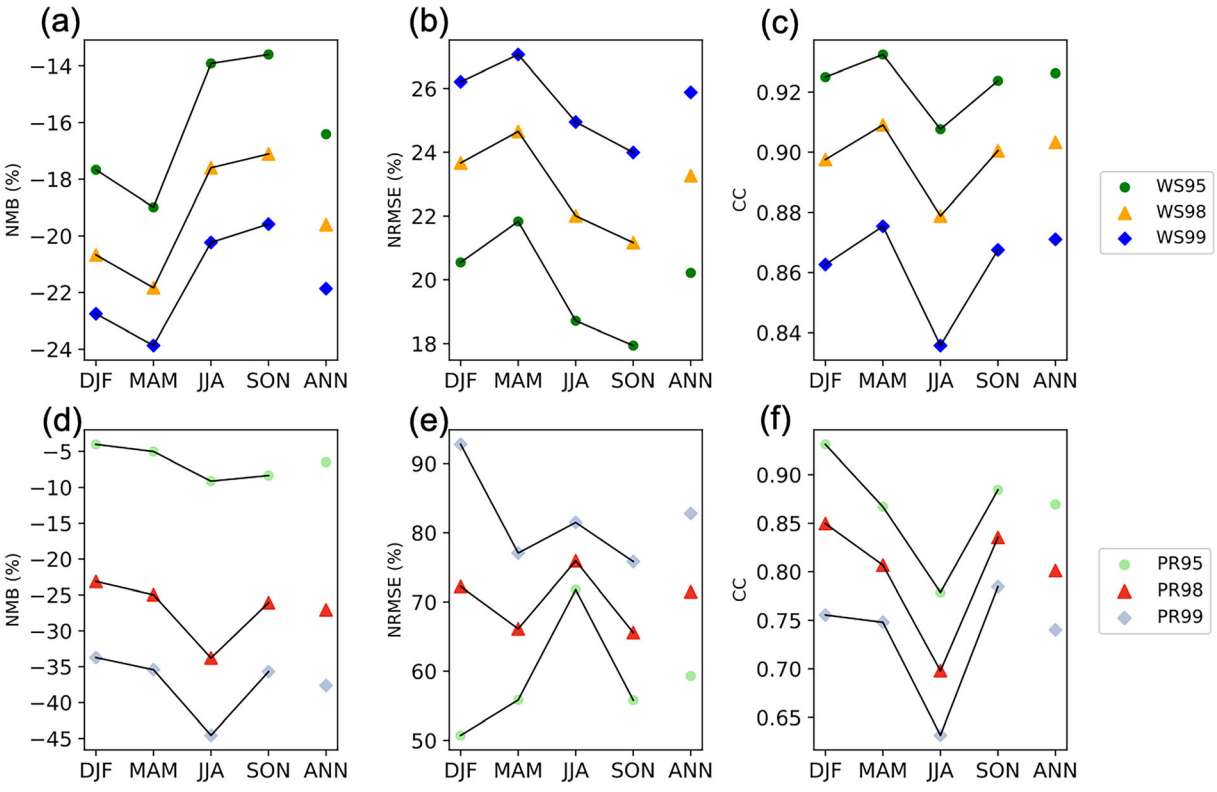

FIGURE 10 Sensitivity of the NRB (left), the NRMSE (middle) and the CC (right) to the definition of extreme wind speeds (top panels) and precipitation (bottom panels) within ETCs. Three quantile values are used to assess the sensitivity: 95th, 98th and 99th. [Colour figure can be viewed at wileyonlinelibrary.com]

(98th and 99th) within ETC centres (Figure 10). Regardless of the variable, the higher the spatial percentile, the larger the error magnitudes (NMB and NRMSE) and the lower the linear correlation (CC) between ERA5 and ISD for all seasons. This indicates a monotonic decrease in the performance of ERA5 at representing rarer local wind and precipitation extremes within ETCs. The seasonal variation of error metrics mostly remains unchanged when different percentiles are used (except for NMSE for PR98 and PR99). The error is more sensitive to different percentiles for precipitation extremes than for wind speed extremes. For example, the change of annual NMB from 95th to 99th percentiles is about 6% (from −16.4% to −21.9%) for wind and 30% (from −6.5% to −37.7%) for precipitation. This is partially related to the structural disparity in the tails of the distributions for both variables, as extreme precipitation values increase more sharply than wind speed values given the same increment in percentiles.

4.3 | Comparison with previous studies

Our findings regarding ERA5's good performance in the spatially-averaged 10-m wind speeds but a systematic underestimation at moderate and strong intensities are in general agreement with previous studies evaluating ERA5 against the buoy and satellite data over the ocean (e.g., Çalışır et al., 2023; Campos et al., 2022). Campos et al. (2022) reported an underestimation of the long-term mean wind speed by 10%–15% conditioned on the presence of cyclones over the central and western North Atlantic. The value is comparable to our estimation of 17% underestimation based on the annual-mean, ETC-associated WSavg over the continental North America, although slightly smaller. Our results are somewhat contrary to those of Molina et al. (2021), who examined the monthly 10-m wind speed between ERA5 and station data across Europe without pre-conditioning on ETCs. They showed that ERA5 tends to overestimate higher wind speeds in cold months and that ERA5 exhibits a better performance in summer months. The differences from our results may be related to that the reanalysis performance varies for different time scales (e.g., Tan et al., 2017), geographical regions and meteorological conditions (e.g., Campos et al., 2022). Nevertheless, Molina et al.'s (2021) examination using the hourly ERA5 data at the worst-performing stations agrees that ERA5 tends to overestimate light winds and underestimate strong winds, a well-known feature in reanalysis datasets (e.g., Cannon et al., 2015). Our bias maps are also in line with previous works, showing that reanalysis products tend to severely underestimate near-surface wind speed over mountainous regions but overestimation in coastal sites (e.g., Gualtieri, 2022; Minola et al., 2020).

Regarding the ETC-associated precipitation, our results showing an overall underestimation tendency in their intensity are in quantitative agreement with previous studies, although these studies were not conditioned to cyclone events and were focused on different continental regions (e.g., Bandhauer et al., 2022; Lavers et al., 2022; Lei et al., 2022; Singh et al., 2021). Lei et al. (2022) showed that the applicability of ERA5 increases with the precipitation amount and hence ERA5 exhibits a better ability to estimate extreme precipitation in rainy than non-rainy seasons in China. Such results are contrary to our findings as we find the best seasonal performance in DJF when ETCs over North America are characterized by relatively low precipitation due to low moisture content. Interestingly, our PRavg bias map prevailed by relatively strong negative values in JJA bears some resemblance to Lavers et al. (2022, their fig. 2) even though their evaluation was not exclusive to cyclones. Based on the gauged-based precipitation, they noted that while wet biases for the mean daily precipitation are more common over North America, there is a notable dry bias over the central United States in July, which they suggested to be related to the model's uncertainty in irrigation and soil moisture content. Overall, our results are consistent with Lavers et al. (2022) that the capability of ERA5 precipitation in the Northern Hemisphere extratropics reduces from winter to summer.

5 | CONCLUSION

This study provides a novel and comprehensive evaluation of the ability of ERA5 reanalysis at representing the 10-m wind speed and hourly precipitation associated with ETCs over North America. Hourly data collected from approximately 3000 stations, amounting to around 420 million reports stored in the ISD, serve as the reference dataset. To ensure a fair comparison, ERA5 grid points are masked out where and when ISD data were not available, and additional quality control and time resampling are also employed on ISD to be consistent with the regularly-gridded hourly ERA5 data. Such post-processed ISD data has been made publicly available to facilitate future studies (Collet et al., 2022). We use an objective algorithm to identify and track ETCs, and two quantities are computed for each identified cyclone centre: a spatial average and a spatial extreme (the spatial 95th, 98th and 99th percentiles) within a radius of 1000 km.

In terms of the spatial means around cyclones centres, it is shown that ERA5 is able to represent the 10-m wind speeds well, with an annual normalized bias (NMB; ERA5-ISD) and root-mean-square error (NRMSE) of about −0.7% and 14%, and a correlation coefficient (CC) of 0.92. Despite good overall performance, ERA5 consistently overestimates low wind speeds and underestimates high wind speeds. For precipitation, an overall underestimation tendency is observed (except for DJF). The performance of ERA5 is poorer for precipitation than for wind speed in all seasons, with NMB and NRMSE increasing their magnitudes to −10% and 57%, respectively, and the CC dropping to 0.87. Such a result is expected as precipitation is notoriously difficult to properly represent in models and reanalysis products, owing to its nonlinear multiscale nature and its dependency on parameterized processes (Tapiador et al., 2019). For both variables, ERA5 usually exhibits the best and the worst performance during DJF and JJA, respectively, likely related to the inadequacy of coarse-resolution models to simulate convective processes, which are more dominant during summer and less active in winter months. As for the spatial distribution, negative biases are often observed over regions with stronger ETC-associated precipitation/wind speeds, which are generally distributed on the central and eastern North America for precipitation, and near Rockies and northeastern North America (entrance of maritime storm tracks) for wind speed. In addition, systematic underestimation in wind speed also prevails over complex topography.

The evaluation for the top 5% extreme cyclone centres based on the spatial means of wind speed/precipitation show a clear skill degradation of ERA5 compared to its performance for the entire sample of ETCs. For wind speed, the magnitude of NMB increases from −0.7% to −10% and the CC reduces from 0.9 to 0.7. For precipitation, ERA5's skill deteriorates even more with the NMB changes from −10% to −23% and CC drops from 0.9 to 0.3. For the spatial extremes within an ETC, ERA5 shows an even stronger tendency to underestimate the localized extreme values than presenting the spatial means of extreme ETCs, and all error metrics increases at higher spatial percentiles.

Our results highlight some important limitations of the ERA5 reanalysis products for studies looking at possible impacts of ETCs. ERA5 is in general more reliable in presenting ETC-associated 10-m wind speed than precipitation. An overall higher skill in DJF lends confidence in the usage of ERA5 for representing the averaged impacts of wintertime ETCs, while the lower skill in JJA suggests that uncertainty should not be overlooked when investigating summer events with ERA5. The deteriorated performance of ERA5 in representing local extremes within ETCs suggests that such applications should be performed with caution.

AUTHOR CONTRIBUTIONS

Ting-Chen Chen: Writing – original draft; writing – review and editing; investigation; supervision; validation; methodology. **François Collet:** Writing – original draft; writing – review and editing; data curation; investigation; formal analysis; methodology; visualization; validation. **Alejandro Di Luca:** Conceptualization; funding acquisition; writing – review and editing; project administration; resources; supervision; investigation; methodology; validation.

ACKNOWLEDGEMENTS

This research has been conducted as part of the project "Simulation et analyse du climate à haute résolution" funded by the Government of Québec. A. Di Luca was also funded by the Natural Sciences and Engineering Research Council of Canada (NSERC) grant (RGPIN-2020-05631). The authors would like to thank Katja Winger, François Roberge and Frédérik Toupin for maintaining a user-friendly local computing facility and for downloading and preparing some of the precipitation datasets.

DATA AVAILABILITY STATEMENT

The data we post-process in this study have been archived as North America ISD to ERA5 (NA-ISD2ERA) Catalogue and made available on the Borealis data repository (Collet et al., 2022). The observational station data, NOAA Integrated Surface Database (ISD) was accessed from https://registry.opendata.aws/noaa-isd. The ERA5 reanalysis is freely available on the Copernicus Data Store (CDS) at https://cds.climate.copernicus.eu/cdsapp#!/dataset/reanalysis-era5-single-levels?tab=overview (Hersbach et al., 2020).

ORCID

Ting-Chen Chen https://orcid.org/0000-0001-9254-2314
François Collet https://orcid.org/0009-0000-9110-817X

REFERENCES

Arsenault, R., Brissette, F., Martel, J.L., Martel, J.L., Troin, M., Lévesque, G. et al. (2020) A comprehensive, multisource database for hydrometeorological modeling of 14,425 North American watersheds. *Scientific Data*, 7, 243. Available from: https://doi.org/10.1038/s41597-020-00583-2

Bandhauer, M., Isotta, F., Lakatos, M., Lussana, C., Båserud, L., Izsák, B. et al. (2022) Evaluation of daily precipitation analyses in E-OBS (v19.0e) and ERA5 by comparison to regional high-resolution datasets in European regions. *International Journal of Climatology*, 42(2), 727–747. Available from: https://doi.org/10.1002/joc.7269

Bauer, M. & Del Genio, A.D. (2006) Composite analysis of winter cyclones in a GCM: influence on climatological humidity. *Journal of Climate*, 19, 1652–1672. Available from: https://doi.org/10.1175/JCLI3690.1

Booth, J.F., Naud, C.M. & Willison, J. (2018) Evaluation of extratropical cyclone precipitation in the North Atlantic basin: an analysis of ERA-interim, WRF, and two CMIP5 models. *Journal of Climate*, 31(6), 2345–2360. Available from: https://doi.org/10.1175/JCLI-D-17-0308.1

Booth, J.F., Rieder, H.E., Lee, D.E. & Kushnir, Y. (2015) The paths of extratropical cyclones associated with wintertime high-wind events in the Northeastern United States. *Journal of Applied Meteorology and Climatology*, 54, 1871–1885. Available from: https://doi.org/10.1175/JAMC-D-14-0320.1

Brune, S., Keller, J.D. & Wahl, S. (2021) Evaluation of wind speed estimates in reanalyses for wind energy applications. *Advances in Science and Research*, 18, 115–126. Available from: https://doi.org/10.5194/asr-18-115-2021

Çalışır, E., Soran, M.B. & Akpınar, A. (2023) Quality of the ERA5 and CFSR winds and their contribution to wave modelling performance in a semi-closed sea. *Journal of Operational Oceanography*, 16(2), 106–130. Available from: https://doi.org/10.1080/1755876X.2021.1911126

Campos, R.M., Gramcianinov, C.B., de Camargo, R. & da Silva Dias, P.L. (2022) Assessment and calibration of ERA5 severe winds in the Atlantic Ocean using satellite data. *Remote Sensing*, 14, 4918. Available from: https://doi.org/10.3390/rs14194918

Cannon, D., Brayshaw, D., Methven, J., Coker, P. & Lenaghan, D. (2015) Using reanalysis data to quantify extreme wind power generation statistics: a 33 year case study in Great Britain. *Renewable Energy*, 75, 767–778. Available from: https://doi.org/10.1016/j.renene.2014.10.024

Catto, J.L., Ackerley, D., Booth, J.F., Champion, A.J., Colle, B.A., Pfahl, S. et al. (2019) The future of midlatitude cyclones. *Current Climate Change Reports*, 5, 407–420. Available from: https://doi.org/10.1007/s40641-019-00149-4

Catto, J.L., Shaffrey, L.C. & Hodges, K.I. (2010) Can climate models capture the structure of extratropical cyclones? *Journal of Climate*, 23(7), 1621–1635. Available from: https://doi.org/10.1175/2009JCLI3318.1

Chartrand, J. & Pausata, F.S.R. (2020) Impacts of the North Atlantic oscillation on winter precipitations and storm track variability in Southeast Canada and the Northeast United States. *Weather and Climate Dynamics*, 1(2), 731–744. Available from: https://doi.org/10.5194/wcd-1-731-2020

Chen, C. & Knutson, T. (2008) On the verification and comparison of extreme rainfall indices from climate models. *Journal of Climate*, 21, 1605–1621. Available from: https://doi.org/10.1175/2007JCLI1494.1

Chen, T.-C., Di Luca, A., Winger, K., Laprise, R. & Thériault, J.M. (2022) Seasonality of continental extratropical-cyclone wind speeds over northeastern North America. *Geophysical Research Letters*, 49(15), e2022GL098776. Available from: https://doi.org/10.1029/2022GL098776

Chu, H., Luo, X., Ouyang, Z., Chan, W.S., Dengel, S., Biraud, S.C. et al. (2021) Representativeness of Eddy-covariance flux footprints for areas surrounding AmeriFlux sites. *Agricultural and Forest Meteorology*, 301–302, 108350. Available from: https://doi.org/10.1016/j.agrformet.2021.108350

Collet, F., Di Luca, A. & Chen, T.-C. (2022) North America ISD to ERA5 (NA-ISD2ERA) Catalogue. https://doi.org/10.5683/SP3/LWMGRM

Copernicus Climate Change Service, Climate Data Store. (2023) *ERA5 hourly data on single levels from 1940 to present*. Copernicus Climate Change Service (C3S) Climate Data Store (CDS). https://doi.org/10.24381/cds.adbb2d47

Di Luca, A., de Elia, R., Bador, M. & Argüeso, D. (2020) Contribution of mean climate to hot temperature extremes for present and future climates. *Weather and Climate Extremes*, 28, 1–13. Available from: https://doi.org/10.1016/j.wace.2020.100255

Di Luca, A., Evans, J.P., Pepler, A., Alexander, L. & Argüeso, D. (2015) Resolution sensitivity of cyclone climatology over Eastern Australia using six reanalysis products. *Journal of Climate*, 28, 9530–9549. Available from: https://doi.org/10.1175/JCLI-D-14-00645.1

Environnement et Changement Climatique Canada. (2021) *Manuel des normes d'observations météorologiques de surface (MANOBS)*. Available from https://www.canada.ca/fr/environnement-changement-climatique/services/manuels-documents-conditions-meteorologiques/manobs-observations-surface.html#toc0

European Centre for Medium-Range Weather Forecasts. (2016) IFS documentation CY41R2—part IV: physical processes. In: *IFS documentation CY41R2*. Reading, UK: ECMWF. Available from: https://doi.org/10.21957/tr5rv27xu

Feser, F., Barcikowska, M., Krueger, O., Schenk, F., Weisse, R. & Xia, L. (2015) Storminess over the North Atlantic and northwestern Europe—a review. *Quarterly Journal of the Royal Meteorological Society*, 141, 350–382. Available from: https://doi.org/10.1002/qj.2364

Field, P.R. & Wood, R. (2007) Precipitation and cloud structure in midlatitude cyclones. *Journal of Climate*, 20(2), 233–254. Available from: https://doi.org/10.1175/JCLI3998.1

Government of Canada. (2020) Canada's top 10 weather stories of 2019. Available from: https://www.canada.ca/en/environment-climate-change/services/top-ten-weather-stories/2019.html#toc8 [Accessed 7th October 2023].

Gualtieri, G. (2022) Analysing the uncertainties of reanalysis data used for wind resource assessment: a critical review. *Renewable and Sustainable Energy Reviews*, 167, 112741. Available from: https://doi.org/10.1016/j.rser.2022.112741

Hawcroft, M.K., Shaffrey, L.C., Hodges, K.I. & Dacre, H.F. (2012) How much northern hemisphere precipitation is associated with extratropical cyclones? *Geophysical Research Letters*, 39(24), L24809. Available from: 10.1029/2012GL053866

Hénin, R., Ramos, A.M., Pinto, J.G. & Liberato, M.L.R. (2021) A ranking of concurrent precipitation and wind events for the Iberian Peninsula. *International Journal of Climatology*, 41, 1421–1437. Available from: https://doi.org/10.1002/joc.6829

Hersbach, H., Bell, B., Berrisford, P., Hirahara, S., Horányi, A., Muñoz-Sabater, J. et al. (2020) The ERA5 global reanalysis. *Quarterly Journal of the Royal Meteorological Society*, 146(730), 1999–2049. Available from: https://doi.org/10.1002/qj.3803

Hodges, K.I., Lee, R.W. & Bengtsson, L. (2011) A comparison of extratropical cyclones in recent reanalyses ERA-interim, NASA MERRA, NCEP CFSR, and JRA-25. *Journal of Climate*,

24(18), 4888–4906. Available from: https://doi.org/10.1175/2011JCLI4097.1

Hoskins, B.J. (1990) Theory of extratropical cyclones. In: Newton, C.W. & Holopainen, E.O. (Eds.) *Extratropical cyclones*. Boston, MA: American Meteorological Society. Available from: https://doi.org/10.1007/978-1-944970-33-8_5

Insurance Bureau of Canada. (2019) Halloween storm across Eastern Canada caused over $250 million in insured damage. Available from: chrome-extension://efaidnbmnnnibpcajpcglclefindmkaj/https://bac-quebec.qc.ca/media/5487/20191210_press-release_nr-eastern-canada-fall-storms.pdf [Accessed 7th October 2023].

Jeyaratnam, J., Booth, J.F., Naud, C.M., Luo, Z.J. & Homeyer, C.R. (2020) Upright convection in extratropical cyclones: a survey using ground-based radar data over the United States. *Geophysical Research Letters*, 47, e2019GL086620. Available from: https://doi.org/10.1029/2019GL086620

Jiao, D., Xu, N., Yang, F. & Xu, K. (2021) Evaluation of spatial-temporal variation performance of ERA5 precipitation data in China. *Scientific Reports*, 11(1), 17956. Available from: https://doi.org/10.1038/s41598-021-97432-y

Jiménez, P.A., García-Bustamante, E., González-Rouco, J.F., Valero, F., Montávez, J.P. & Navarro, J. (2008) Surface wind regionalization in complex terrain. *Journal of Applied Meteorology and Climatology*, 47, 308–325. Available from: https://doi.org/10.1175/2007JAMC1483.1

Kunkel, K.E., Easterling, D.R., Kristovich, D.A.R., Gleason, B., Stoecker, L. & Smith, R. (2012) Meteorological causes of the secular variations in observed extreme precipitation events for the conterminous United States. *Journal of Hydrometeorology*, 13, 1131–1141. Available from: 10.1175/JHM-D-11-0108.1

Lavers, D.A., Simmons, A., Vamborg, F. & Rodwell, M.J. (2022) An evaluation of ERA5 precipitation for climate monitoring. *Quarterly Journal of the Royal Meteorological Society*, 148(748), 3124–3137. Available from: https://doi.org/10.1002/qj.4351

Lei, X., Xu, W., Chen, S., Yu, T., Hu, Z., Zhang, M. et al. (2022) How well does the ERA5 reanalysis capture the extreme climate events over China? Part I: extreme precipitation. *Frontiers in Environmental Science*, 10, 921658. Available from: https://doi.org/10.3389/fenvs.2022.921658

Lin, Y. & Mitchell, K.E. (2005) The NCEP stage II/IV hourly precipitation analyses: development and applications. In: *Preprints. 19th conference on hydrology*. San Diego, CA: American Meteorological Society. Available from: https://ams.confex.com/ams/pdfpapers/83847.pdf

Lott, J.N. (2004) *The quality control of the integrated surface hourly database*. Seattle, WA: American Meteorological Society.

Minola, L., Zhang, F., Azorin-Molina, C., Pirooz, A.A.S., Flay, R.G.J., Hersbach, H. et al. (2020) Near-surface mean and gust wind speeds in ERA5 across Sweden: towards an improved gust parametrization. *Climate Dynamics*, 55(3–4), 887–907. Available from: https://doi.org/10.1007/s00382-020-05302-6

Molina, M.O., Gutiérrez, C. & Sánchez, E. (2021) Comparison of ERA5 surface wind speed climatologies over Europe with observations from the HadISD dataset. *International Journal of Climatology*, 41(10), 4864–4878. Available from: https://doi.org/10.1002/joc.7103

Naud, C.M., Booth, J.F., Lebsock, M. & Grecu, M. (2018) Observational constraint for precipitation in extratropical cyclones: sensitivity to data sources. *Journal of Applied Meteorology and Climatology*, 57, 991–1009. Available from: https://doi.org/10.1175/JAMC-D-17-0289.1

Naud, C.M., Jeyaratnam, J., Booth, J.F., Zhao, M. & Gettelman, A. (2020) Evaluation of modeled precipitation in oceanic extratropical cyclones using IMERG. *Journal of Climate*, 33, 95–113. Available from: https://doi.org/10.1175/JCLI-D-19-0369.1

Nelson, B.R., Prat, O.P., Seo, D. & Habib, E. (2016) Assessment and implications of NCEP stage IV quantitative precipitation estimates for product intercomparisons. *Weather and Forecasting*, 31, 371–394. Available from: 10.1175/WAF-D-14-00112.1

Neu, U., Akperov, M.G., Bellenbaum, N., Benestad, R., Blender, R., Caballero, R. et al. (2013) Imilast: a community effort to intercompare extratropical cyclone detection and tracking algorithms. *Bulletin of the American Meteorological Society*, 94(4), 529–547. Available from: https://doi.org/10.1175/BAMS-D-11-00154.1

NOAA (1998) Automated Surface Observing System: User's guide. *National Oceanic and Atmospheric Administration Doc.*, 61 pp. Available at: https://www.weather.gov/media/asos/aum-toc.pdf [Accessed: 7th December 2023].

NOAA-National Centers for Environmental Information. (2018) *Federal climate complex data documentation for integrated surface data (ISD)*. Available from: https://www.ncei.noaa.gov/data/global-hourly/doc/isd-format-document.pdf

Owen, L.E., Catto, J.L., Stephenson, D.B. & Dunstone, N.J. (2021) Compound precipitation and wind extremes over Europe and their relationship to extratropical cyclones. *Weather and Climate Extremes*, 33, 100342. Available from: https://doi.org/10.1016/j.wace.2021.100342

Peña-Arancibia, J.L., van Dijk, A.I.J.M., Renzullo, L.J. & Mulligan, M. (2013) Evaluation of precipitation estimation accuracy in reanalyses, satellite products, and an ensemble method for regions in Australia and south and East Asia. *Journal of Hydrometeorology*, 14(4), 1323–1333 https://journals.ametsoc.org/view/journals/hydr/14/4/jhm-d-12-0132_1.xml

Pepler, A., Di Luca, A. & Evans, J.P. (2018) Independently assessing the representation of midlatitude cyclones in high-resolution reanalyses using satellite observed winds. *International Journal of Climatology*, 38, 1314–1327. Available from: https://doi.org/10.1002/joc.5245

Petterssen, S. & Smebye, S.J. (1971) On the development of extratropical cyclones. *Quarterly Journal of the Royal Meteorological Society*, 97, 457–482.

Plante, M., Son, S.W., Atallah, E., Gyakum, J. & Grise, K. (2015) Extratropical cyclone climatology across eastern Canada. *International Journal of Climatology*, 35(10), 2759–2776. Available from: https://doi.org/10.1002/joc.4170

Poan, E.D., Gachon, P., Laprise, R., Aider, R. & Dueymes, G. (2018) Investigating added value of regional climate modeling in north American winter storm track simulations. *Climate Dynamics*, 50(5–6), 1799–1818. Available from: https://doi.org/10.1007/s00382-017-3723-9

Reitan, C.H. (1974) Frequencies of Cyclones and Cyclogenesis for North America, 1951–1970. *Monthly Weather Review*, 102, 861–868. Available from: https://doi.org/10.1175/1520-0493(1974)102<0861:FOCACF>2.0.CO;2

Rudeva, I. & Gulev, S.K. (2011) Composite analysis of North Atlantic extratropical cyclones in NCEP–NCAR reanalysis data.

Monthly Weather Review, 139, 1419–1446. Available from: https://doi.org/10.1175/2010MWR3294.1

Sandu, I., Zadra, A. & Wedi, N. (n.d.) *Impact of orographic drag on forecast skill*. Available from: https://www.ecmwf.int/en/newsletter/150/meteorology/impact-orographic-drag-forecast-skill [Accessed 29th August 2022].

Serreze, M.C., Lynch, A.H. & Clark, M.P. (2001) The Arctic frontal zone as seen in the NCEP–NCAR reanalysis. *Journal of Climate*, 14(7), 1550–1567. Available from: https://doi.org/10.1175/1520-0442(2001)014<1550:TAFZAS>2.0.CO;2

Simmonds, I. & Keay, K. (2000) Mean southern hemisphere extratropical cyclone behavior in the 40-year NCEP–NCAR reanalysis. *Journal of Climate*, 13, 873–885. Available from: https://doi.org/10.1175/1520-0442(2000)013<0873:MSHECB>2.0.CO;2

Sinclair, V.A., Rantanen, M., Haapanala, P., Räisänen, J. & Järvinen, H. (2020) The characteristics and structure of extra-tropical cyclones in a warmer climate. *Weather and Climate Dynamics*, 1(1), 1–25. Available from: https://doi.org/10.5194/wcd-1-1-2020

Singh, T., Saha, U., Prasad, V.S. & Gupta, M.D. (2021) Assessment of newly-developed high resolution reanalyses (IMDAA, NGFS and ERA5) against rainfall observations for Indian region. *Atmospheric Research*, 259, 105679. Available from: https://doi.org/10.1016/j.atmosres.2021.105679

Smith, A., Lott, N. & Vose, R. (2011) The integrated surface database: recent developments and partnerships. *Bulletin of the American Meteorological Society*, 92(6), 704–708. Available from: https://doi.org/10.1175/2011BAMS3015.1

Sorteberg, A. & Walsh, J.E. (2008) Seasonal cyclone variability at 70°N and its impact on moisture transport into the Arctic. *Tellus A*, 60, 570–586. Available from: https://doi.org/10.1111/j.1600-0870.2008.00314.x

Tan, J., Petersen, W.A., Kirstetter, P.-E. & Tian, Y. (2017) Performance of IMERG as a function of spatiotemporal scale. *Journal of Hydrometeorology*, 18, 307–319. Available from: https://doi.org/10.1175/JHM-D-16-0174.1

Tapiador, F.J., Roca, R., Del Genio, A., Dewitte, B., Petersen, W. & Zhang, F. (2019) Is precipitation a good metric for model performance? *Bulletin of the American Meteorological Society*, 100, 223–233. Available from: https://doi.org/10.1175/BAMS-D-17-0218.1

Uccellini, L.W. (1990) Processes contributing to the rapid development of extratropical cyclones. In: Newton, C.W. & Holopainen, E.O. (Eds.) *Extratropical Cyclones*. Boston, MA: American Meteorological Society. Available from: https://doi.org/10.1007/978-1-944970-33-8_6

Vaisala. (2020) Wind sensor WM30 for mobile applications. Available from: https://www.vaisala.com/sites/default/files/documents/WM30-datasheet-B210384EN.pdf [Accessed: 3rd November 2023].

Vaisala. (2021) Rain gauge QMR101 and QMR101. Available from: https://www.vaisala.com/sites/default/files/documents/QMR101-QMR101M-Datasheet-B211713EN.pdf [Accessed: 3rd November 2023].

Wang, X.L., Feng, Y., Chan, R. & Isaac, V. (2016) Inter-comparison of extra-tropical cyclone activity in nine reanalysis datasets. *Atmospheric Research*, 181, 133–153. Available from: https://doi.org/10.1016/j.atmosres.2016.06.010

Wang, X.L., Swail, V.R. & Zwiers, F.W. (2006) Climatology and changes of extratropical cyclone activity: comparison of ERA-40 with NCEP–NCAR reanalysis for 1958–2001. *Journal of Climate*, 19, 3145–3166. Available from: https://doi.org/10.1175/JCLI3781.1

Zappa, G., Shaffrey, L.C. & Hodges, K.I. (2013) The ability of CMIP5 models to simulate North Atlantic extratropical cyclones. *Journal of Climate*, 26, 5379–5396.

SUPPORTING INFORMATION

Additional supporting information can be found online in the Supporting Information section at the end of this article.

How to cite this article: Chen, T.-C., Collet, F., & Di Luca, A. (2024). Evaluation of ERA5 precipitation and 10-m wind speed associated with extratropical cyclones using station data over North America. *International Journal of Climatology*, 1–19. https://doi.org/10.1002/joc.8339